Ecological Indicators 67 (2016) 788–797

Contents lists available at ScienceDirect

Ecological Indicators

journal homepage: www.elsevier.com/locate/ecolind

Drought-induced dynamics of carbon and water use efficiency of global grasslands from 2000 to 2011

Chengcheng Gang[a,b,*], Zhaoqi Wang[c], Yizhao Chen[c], Yue Yang[c], Jianlong Li[c], Jimin Cheng[a,b], Jiaguo Qi[d], Inakwu Odeh[e]

[a] Institute of Soil and Water Conservation, Northwest A&F University, Yangling 712100, China
[b] Institute of Soil and Water Conservation, Chinese Academy of Sciences and Ministry of Water Resources, Yangling 712100, China
[c] The Global Change Research Institute, School of Life Sciences, Nanjing University, Nanjing 210093, China
[d] The Center for Global Change & Earth Observations, Michigan State University, East Lansing 48824, USA
[e] Department of Environmental Science, Faculty of Agricultural and Environment, The University of Sydney, Sydney 2006, Australia

ARTICLE INFO

Article history:
Received 30 October 2015
Received in revised form 21 February 2016
Accepted 26 March 2016
Available online 25 April 2016

Keywords:
Carbon use efficiency (CUE)
Drought Severity Index (DSI)
Drought conditions
Global grassland ecosystems
Water use efficiency (WUE)

ABSTRACT

Drought is frequently recorded as a result of climate warming and elevated concentration of greenhouse gases, which affect the carbon and water cycles in terrestrial ecosystems, particularly in arid and semi-arid regions. To identify the drought in grassland ecosystems and to determine how such drought affects grassland ecosystems in terms of carbon and water cycles across the globe, this study evaluated the drought conditions of global grassland ecosystems from 2000 to 2011 on the basis of the remotely sensed Drought Severity Index (DSI) data. The temporal dynamics of grassland carbon use efficiency (CUE) and water use efficiency (WUE), as well as their correlations with DSI, were also investigated at the global scale. Results showed that 57.04% of grassland ecosystems experienced a dry trend over this period. In general, most grassland ecosystems in the northern hemisphere (N.H.) were in near normal condition, whereas those in the southern hemisphere (S.H.) experienced a clear drying and wetting trend, with the year 2005 regarded as the turning point. Grassland CUE increased continually despite the varied drought conditions over this period. By contrast, WUE increased in the closed shrublands and woody savannas but decreased in all the other grassland types. The drought conditions affected the carbon and water use mainly by influencing the primary production and evapotranspiration of grass through photosynthesis and transpiration process. The CUE and WUE of savannas was most sensitive to droughts among all the grassland types. The areas of grassland DSI that showed significant correlations with CUE and WUE were 52.92% and 22.11% of the total grassland areas, respectively. Overall, droughts sufficiently explained the dynamics of grassland CUE, especially in the S.H. In comparison with grassland CUE, the grassland WUE was less sensitive to drought conditions at the global scale.

1. Introduction

Water resources are essential for society and ecosystems. Increasing evidence indicates that the recent climate change has exacerbated the water resources stress by increasing water demand and shrinking water supplies. This condition has strong adverse effects on food security and poses great challenges to the sustainability of life (Vörösmarty et al., 2000; Rosegrant et al., 2003). Drought is an important adverse climate disturbance that is occurred globally, and it is expected to intensify in this century (IPCC, 2007, 2012). Droughts affect the terrestrial carbon and water cycles by reducing the carbon sequestration ability and aggravating the evaporation rate of ecosystems (Ciais et al., 2005; Van der Molen et al., 2011; Battipaglia et al., 2014). Carbon use efficiency (CUE), which is the ratio of net primary productivity (NPP) to gross primary productivity (GPP), and water use efficiency (WUE), which is the ratio of NPP to evapotranspiration (ET), are important indicators for addressing the interactions between the water and carbon cycles of terrestrial ecosystems (Webb et al., 1978; LeHouerou, 1984; Delucia et al., 2007). Several studies have evaluated the effects of climate variables on the CUE and WUE of ecosystems at

* Corresponding author at: Institute of Soil and Water Conservation, Northwest A&F University, Xinong Road 26, Yangling 712100, China. Tel.: +86 29 87081432.
E-mail address: gangcheng024@gmail.com (C. Gang).

http://dx.doi.org/10.1016/j.ecolind.2016.03.049
1470-160X/

multiple scales (Keenan et al., 2013; Adiredjo et al., 2014; Rowland et al., 2014; Zhang et al., 2014). Knowledge has advanced since the development of remote sensing technology with respect to the potential effects of climate change and other drivers on carbon and water cycles at large scales. Although the severity of droughts has been investigated extensively, its subsequent influences on terrestrial CUE and WUE are not well explored. Therefore, monitoring the extent and duration of droughts accurately and consistently is necessary, especially when assessing impacts and mitigating the distresses at global and regional scales.

Many indices have been developed to assess and monitor the occurrence of droughts from regional to global scale, e.g. the Standardized Precipitation Index (SPI) (McKee et al., 1995), the Palmer Drought Severity Index (PDSI) (Palmer, 1965), the Temperature-Vegetation Dryness Index (TVDI) (Sandholt et al., 2002), the Vegetation, Water and Thermal Stress Index (VWTCI) (Shakya and Yamaguchi, 2010). Developed by Mu et al. (2013), the Drought Severity Index (DSI), is an index that combines the meteorological and agricultural drought conditions. It is calculated on the basis of MODIS-derived Normalized Difference Vegetation Index (NDVI) and evapotranspiration/potential evapotranspiration (ET/PET) data with fine resolution at the global scale (Mu et al., 2013). The available DSI dataset extends from 2000 to 2011, and has been validated to capture the major droughts over the last decade worldwide (Zhao and Running, 2010; Mu et al., 2013; Zhang and Yamaguchi, 2014). Given on this, in the present study, the DSI data were used to monitor the extent and duration of drought spread in grassland ecosystems, as well as the effects of such drought spread on the water and carbon cycles of grassland ecosystems at the global scale.

Grassland ecosystems are among the largest distributed biomes, which occupy more than 30% of the Earth's land surface. Grasslands contribute significantly to food security by providing food for ruminants, which serve as sources of meat and milk for human consumption (Scurlock and Hall, 1998; O'Mara, 2012). Grassland ecosystems play a key role in balancing the global atmospheric greenhouse gases through the carbon and water cycles (French, 1979; O'Mara, 2012). Given that grassland ecosystems are mainly distributed in arid and semi-arid regions, temperature and precipitation are two key factors that control the growth and productivity of grass (Gang et al., 2015a,b). With the increasing frequency of climate extremes in recent decades, the effects of droughts on the structure, composition, and function of grassland ecosystems have been widely studied (Wolf et al., 2013; Bollig and Feller, 2014; Burri et al., 2014; Koerner and Collins, 2014; Manea and Leishman, 2014). Short-term droughts are likely to induce the plastic adjustment of the resident plants, whereas long-term progressive droughts would cause the species turnover within plant communities (Helmuth et al., 2005; Jung et al., 2014). However, most of these studies were conducted at the stand or local scale, hence, the understanding on how droughts affect the carbon and water use of grassland ecosystems, especially at the global scale, remain limited. This lack of extensive research represents an important knowledge gap.

The past decade was the warmest 10 years since the instrumental measurements of temperatures began in the 1880s (Zhao and Running, 2010). To address the aforementioned scientific problems during the "warmest decade", the present study primarily aims: (i) to characterize the extent and duration of drought occurred in global grassland ecosystems from 2000 to 2011 by using the remotely sensed DSI data; (ii) to quantify the annual changes in grassland GPP, NPP, ET, CUE, and WUE at the global scale during this period; and (iii) to calculate the correlations between grassland CUE, WUE and DSI, as well as the mean annual temperature (MAT) and mean annual precipitation (MAP), to reflect the how the grassland carbon and water use is controlled by environmental variables. The outcomes of this study do not only elucidate the extent and duration of droughts in global grassland ecosystems in recent years but also provide baselines for enhancing the sustainable carbon and water use in grasslands across the globe. In addition, the findings of this study may serve as guidelines for government and policy makers in initiating adaptation strategies to respond to the climate change and to manage grassland production.

2. Materials and methods

2.1. MODIS DSI, GPP, NPP, and ET data

Annual MODIS DSI, GPP, NPP and ET data (~1 km resolution) extending from 2000 to 2011 were obtained from the Numerical Terra dynamic Simulation Group at the University of Montana (http://www.ntsg.umt.edu/). These dataset are in TIFF format and the WGS84 geographic coordinate system, and were converted into a grid format.

For the remotely sensed DSI data, the ET/PET and snow-free growing season NDVI products of MODIS for all vegetated land areas from 2000 to 2011 were integrated with a 0.05° spatial resolution. The MODIS NDVI is sensitive to vegetation drought responses and associated water stress, especially in the water-limited regions. This situation provides a link between climate change and vegetation responses through greenness changes (Atkinson et al., 2011; Mu et al., 2013). The NDVI product has been successfully used to monitor the global vegetation photosynthetic activities (Huete et al., 2002; Justice et al., 2002). DSI is calculated as a standardized value, which is expressed as follows:

$$A_{\mathrm{NDVI}} = \frac{\mathrm{NDVI} - \overline{\mathrm{NDVI}}}{\delta_{\mathrm{NDVI}}} \quad (1)$$

$$A_{\mathrm{EVA}} = \frac{(\mathrm{ET/PET}) - \overline{(\mathrm{ET/PET})}}{\delta_{(\mathrm{ET/PET})}} \quad (2)$$

$$A = A_{\mathrm{NDVI}} + A_{\mathrm{EVA}} \quad (3)$$

$$\mathrm{DSI} = \frac{A - \overline{A}}{\delta_A} \quad (4)$$

where A_{NDVI} is the standardized anomaly of the NDVI, which is calculated using the long-term mean value of $\overline{\mathrm{NDVI}}$ and the standard deviation δ_{NDVI} of the period 2000–2011; A_{EVA} is the standardized anomaly of ET/PET, which is calculated as the long-term mean value of $\overline{\mathrm{ET/PET}}$ and a standard deviation $\delta_{(\mathrm{ET/PET})}$; ET/PET is the ratio of ET to PET; A is a sum of A_{NDVI} and A_{EVA}; the DSI is a standardized anomaly of A; $\overline{A}$ is the long-term mean value of A_{NDVI} and $A_{(\mathrm{ET/PET})}$; δ_A is the standardized deviation. The categories of drought conditions based on DSI value is shown in Table 1 (Mu et al., 2013).

Table 1
The categories for drought conditions of the global DSI (Mu et al., 2013).

Category	Description	DSI
D5	Extremely drought	<−1.50
D4	Severe drought	−1.49 to −1.20
D3	Moderate drought	−1.99 to −0.9
D2	Mild drought	−0.89 to −0.60
D1	Incipient drought	−0.59 to −0.30
WD	Near normal	−0.29 to 0.29
W1	Incipient wet	0.30 to 0.59
W2	Slightly wet	0.60 to 0.89
W3	Moderately wet	0.90 to 1.19
W4	Very wet	1.20 to 1.50
W5	Extremely wet	>1.50

The three input dataset sources, namely, biome types, the meteorological data, and cloud contaminated MODIS FPAR/LAI data, are the main error sources in the original version of the MODIS algorithm. To reduce these uncertainties, Zhao et al. (2005) reprocessed the key input data set and consequently improved these estimates. First, the meteorological data with coarse resolution input was spatially interpolated to the MODIS pixel level. Second, the missing data in MODIS FPAR/LAI resulting from cloud contamination and malfunction of the MODIS sensor were temporally filled. Furthermore, the Biome Parameter Look-Up Table was recalibrated according to the recent synthesized NPP data and GPP data derived from flux tower measurements. The improved global MODIS primary production products have been widely used to monitor ecological conditions, natural resources, and environmental changes (Zhao et al., 2006; Zhao and Running, 2010; Zhang et al., 2014). The MODIS GPP values are calculated as follows:

$$\mathrm{GPP} = \varepsilon_{\max} \times 0.45 \times \mathrm{SW}_{\mathrm{rad}} \times \mathrm{FPAR} \times fVPD \times fT_{\min} \quad (5)$$

where $\varepsilon_{\max}$ is the maximum light use efficiency under optimal conditions; $\mathrm{SW}_{\mathrm{rad}}$ is the incoming short-wave solar radiation, of which 45% is Photosynthetically Active Radiation (PAR); FPAR is the fraction of PAR absorbed by the plant canopy; *fVPD* is vapour pressure deficits scalar, and $fT_{\min}$ is the daily minimum temperature ($T_{\min}$, °C) scalar.

The MODIS NPP is defined as the difference between GPP and respiration, including maintenance and growth components. The newly developed NPP is calculated as follows:

$$\mathrm{NPP} = \sum_{1}^{365} \mathrm{GPP} - R_{m\_lr} - R_{m\_w} - R_g \quad (6)$$

where R_{m_lr} is the maintenance respiration from living leaves and fine roots, and R_{m_w} is the annual maintenance respiration from living wood, R_g is annual growth respiration. More detailed description for modeling MODIS GPP and NPP can be found in related publications (Zhao et al., 2005, 2006; Zhao and Running, 2011).

The MODIS ET dataset represents transpiration by vegetation and evaporation from canopy and soil surfaces. This dataset is based on the Penman-Monteith equation (Monteith, 1965; Mu et al., 2007a,b). The original version of the ET algorithm does not consider the evaporation from the intercepted precipitation from plant canopy (Mu et al., 2011). The newly developed and improved MODIS ET dataset recalculates the fraction of vegetation cover, the soil heat flux, the canopy water loss, the soil evaporation, the stomatal conductance, aerodynamic resistance, and boundary layer resistance (Mu et al., 2011). The ET algorithm is computed as follows:

$$\lambda E = \lambda E_{wet\_C} + \lambda E_{trans} + \lambda E_{\mathrm{SOIL}} \quad (7)$$

where λE is the total daily ET, λE_{wet_C} is evaporation from the wet canopy surface, λE_{trans} is the transpiration from the dry canopy surface, and $\lambda E_{\mathrm{SOIL}}$ is the evaporation from the soil surface (Mu et al., 2007a,b, 2011). The MODIS ET product has been validated and shows well consistence with daily ET estimation from tower eddy covariance measurements covering a wide range of biomes and climate conditions. The ET data has been used in a wide variety of regional and global research (Mu et al., 2011; Gang et al., 2015a,b). In this study, the annual global ET datasets from 2000 to 2011 was used in WUE calculation. Grassland WUE for each grid cell was calculated as the ratio of annual NPP to ET in the grid.

2.2. Land cover data and climate factors data

The global grassland cover data was derived from the International Geosphere-Biosphere Project (IGBP) land cover dataset, in which 17 land cover classes were identified (Loveland et al., 2000). The grassland cover includes closed shrublands, open shrublands, woody savannas, savannas, and non-woody grasslands (White et al., 2000). The largest distributed grassland type is open shrublands, which account for 32.81% of total grasslands. The closed shrublands is the least distributed grassland type, taking up to 4.10% of total grasslands. The area of woody savannas, savannas and non-woody savannas account for 22.67%, 14.66% and 25.75% of total grassland cover, respectively.

The meteorological data (temperature and precipitation) from 2000 to 2011 were obtained from the Climate Research Unit at the University of East Anglia (Harris et al., 2014). This dataset is provided by the British Atmospheric Data Centre. The mean annual temperature (MAT) and mean annual precipitation (MAP) were incorporated from the monthly data.

2.3. Analysis of grassland DSI dynamic

The ordinary least square estimation was calculated for each pixel to quantify the variations of grassland DSI at a global scale (Gang et al., 2015a,b):

$$Slope = \frac{n \times \sum_{i=1}^{n} i \times DSI_i - \left(\sum_{i=1}^{n} i\right)\left(\sum_{i=1}^{n} DSI_i\right)}{n \times \sum_{i=1}^{n} i^2 - \left(\sum_{i=1}^{n} i\right)^2} \quad (8)$$

where i is 1 for year 2000, 2 for year 2001, . . . n, $n = 12$ as the study period from 2000 to 2011; DSI_i is the value of annual grassland DSI in time of i, $i = 1, \ldots, n$, $n = 12$. If *Slope* in Eq. (8) is positive, it indicates the wet trend, in comparison to negative value which connotes the dry trend.

In addition, the temporal dynamics of the GPP, NPP, ET, DSI, CUE, and WUE for each grassland type from 2000 to 2011 were explored, their annual mean values were plotted against time to estimate the annual changing rate.

2.4. Correlation analysis between grassland CUE, WUE and climate variables

The Pearson correlation coefficients between grassland CUE, WUE and climate variables, including DSI, MAP and MAT were calculated to reflect the sensitivity of grassland CUE and WUE to climate variables. If the correlation coefficient passes the significance test, then an extremely significant ($p < 0.01$) or significant ($p < 0.05$) linear correlation is indicated.

3. Results

3.1. Drought characteristic of global grassland ecosystems

On average, grassland regions in dry condition during the study period accounted for 39.76% of the total grassland areas across the globe, such value is slightly larger than that under wet conditions. Regions in near normal conditions accounted for 22.18% of the total grassland areas. In the N.H., grassland areas in dry conditions (38.88%) were close to those in wet conditions (38.90%). By contrast, in the S.H., 41.96% of the grassland ecosystems experienced drought conditions, whereas 36.42% experienced wet conditions. During the period of 2000–2011, 57.04% of regions vegetated by grassland ecosystems became increasingly dry. These regions are mainly located in Asia, north of North America, southern Africa, and Western Australia (Fig. 1A). Nearly 32.81% of the dry regions in 2000 became wet in 2011, with the area under D1 condition undergoing the most significant change (8.50%). In 2011, 31.47% of the wet regions became dry relative to the condition in 2000, with

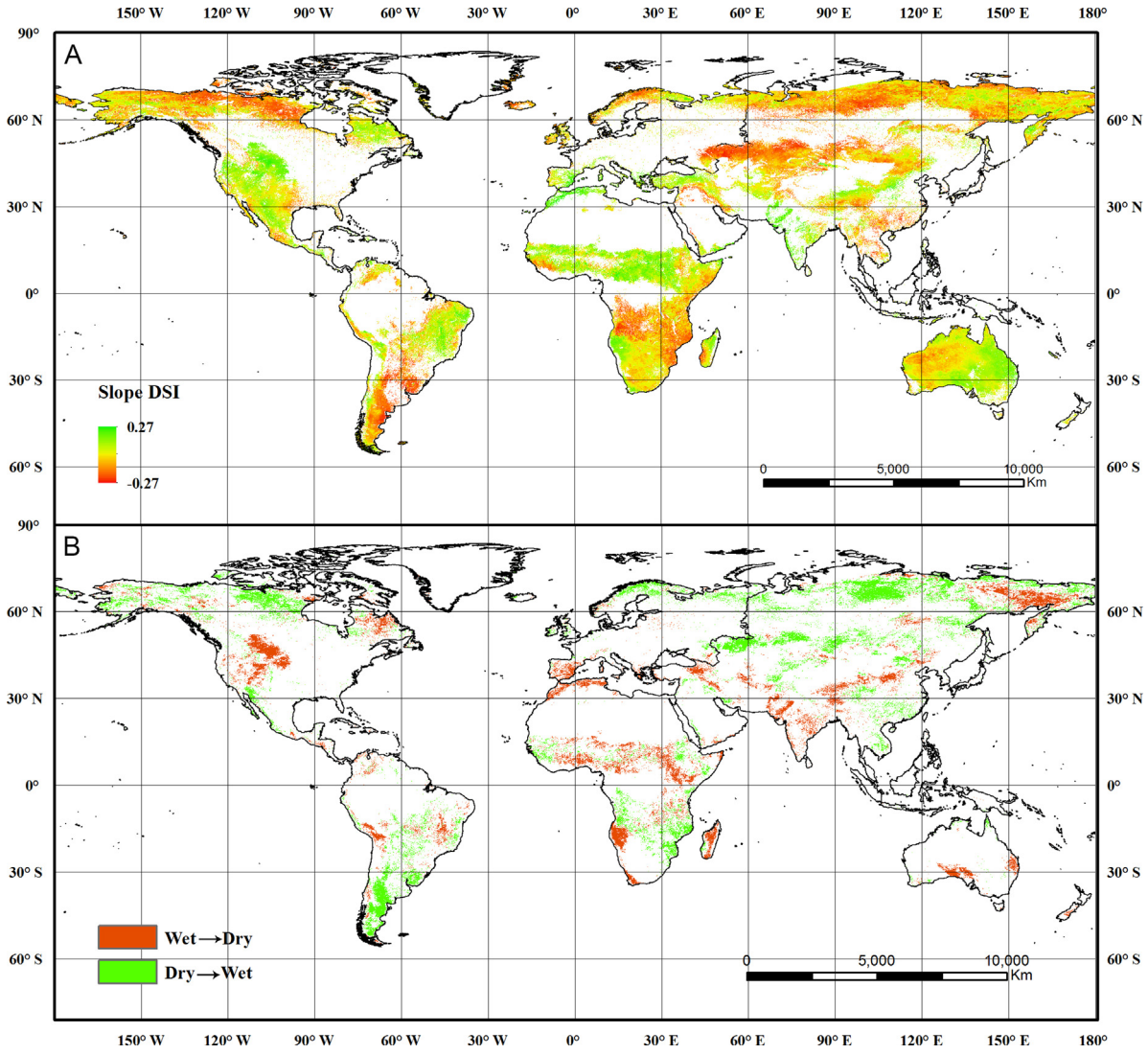

Fig. 1. The spatial pattern of Drought Severity Index (DSI) dynamic (A), the wetting and drying trend (B) of global grassland ecosystems from 2000 to 2011.

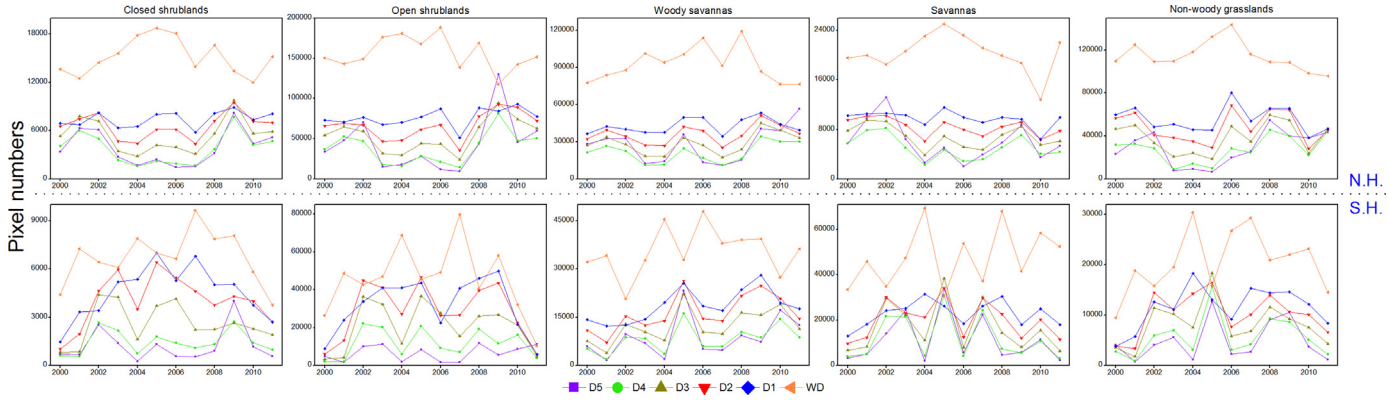

Fig. 2. The area change of each grassland type at different drought levels in the N.H. and the S.H. during 2000–2011. D5: Extremely drought; D4: Severe drought; D3: Moderate drought; D2: Mild drought; D1: Incipient drought; WD: Near normal.

the W1 condition making the most contribution to such change (7.49%) (Fig. 1B). Most of these regions were mainly distributed in the north of the Tropic of Cancer, and the south of the Tropic of Capricorn in the southern America.

In this study, the temporal dynamics of drought conditions for each grassland type were also analyzed. As indicated in Fig. 2, most grassland ecosystems were in near normal condition over the study period. In the N.H., the areas of closed shrublands, open

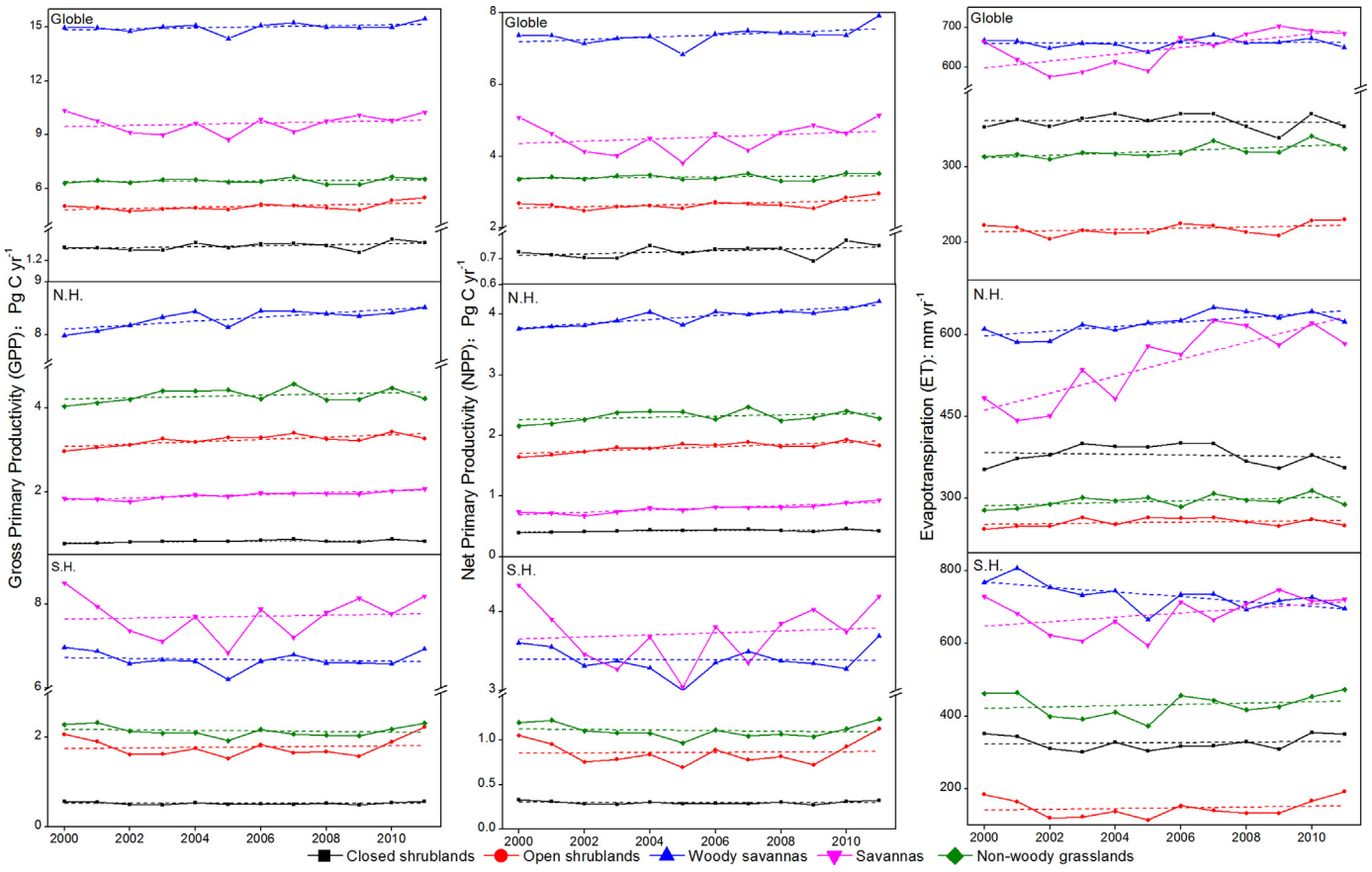

Fig. 3. The temporal dynamics of grassland GPP, NPP, and ET from 2000 to 2011.

shrublands, woody savannas, savannas and non-woody grasslands under near normal condition accounted for 22.15%, 22.03%, 22.43%, 21.85% and 22.65% of the total grassland cover, respectively. The regions that experienced different drought levels showed similar changing trends in the past 12 years. Noticeably, the expansion of extreme drought occurred in all grassland types in 2002 and 2009. In the case of the S.H., the grassland ecosystems in near normal condition accounted 21.37% for closed shrublands, 20.65% for open shrublands, 22.15% for woody savannas, 22.89% for savannas and 21.03% for non-woody grasslands on average. Overall, these areas increased at the first half of the study period, and decreased at the latter half of the study period. Meanwhile, the dry spells expanded gradually before 2005, and decreased thereafter.

3.2. The temporal dynamics of grassland GPP, NPP, ET, DSI, CUE, and WUE

The mean annual values of grassland GPP, NPP, and ET from 2000 to 2011 at the global scale were first evaluated. As indicated in Fig. 3, both of the GPP and NPP of each grassland type increased at the global scale over the entire study period. These increasing trends were also observed in the N. H. By contrast, in the S.H., GPP and NPP increased in open shrublands and savannas, but decreased in all the other grassland types. With regard to the ET, a decreasing trend occurred in the closed shrublands both at the global scale and in the N.H. over the past 12 years, as well as in the woody savannas in the S.H. All the other grassland types showed an ascending ET.

The annual DSI, CUE, and WUE during this period were also plotted against time. Most grasslands at the global scale were in near normal condition from 2000 to 2011 (Fig. 4). The incipient drought occurred in 2002, 2005, and 2009. Savannas experienced a mild drought in 2005. Similarly, grasslands in the N.H. were in near normal condition in most years from 2000 to 2011. The overall variation can be divided into three stages, the wet trend from 2000 to 2004, the dry trend from 2004 to 2009, and the wet recovery trend from 2009 to 2011. In the S.H., the W1 and D1 conditions were frequently recorded in grassland ecosystems. The dry spells expanded fluctuately from 2000 to 2004, but the most severe drought occurred in 2005, after which a gradual recovery was observed. Globally, the CUE of all grassland types increased over the past 12 years. The increase of CUE in the N.H. fluctuated in all grassland types from 2000 to 2011. In the S.H., CUE only increased in the woody savannas and savannas. All the other grassland types showed decreased CUE over this period. Noticeably, the temporal dynamic of grassland CUE in the S.H. was closely related to the changing pattern of DSI. For the WUE, the closed shrublands and woody savannas showed an overall increasing WUE globally from 2000 to 2011. By contrast, all the other grassland types showed decreased WUE over this period. The closed and open shrublands in the N.H. presented an ascending trend during the past 12 years. Before 2005, the WUE of savannas changed drastically in comparison with the WUE values of the other grassland types. By contrast, in the S.H., the WUE decreased in all the grassland types, except in the woody savannas.

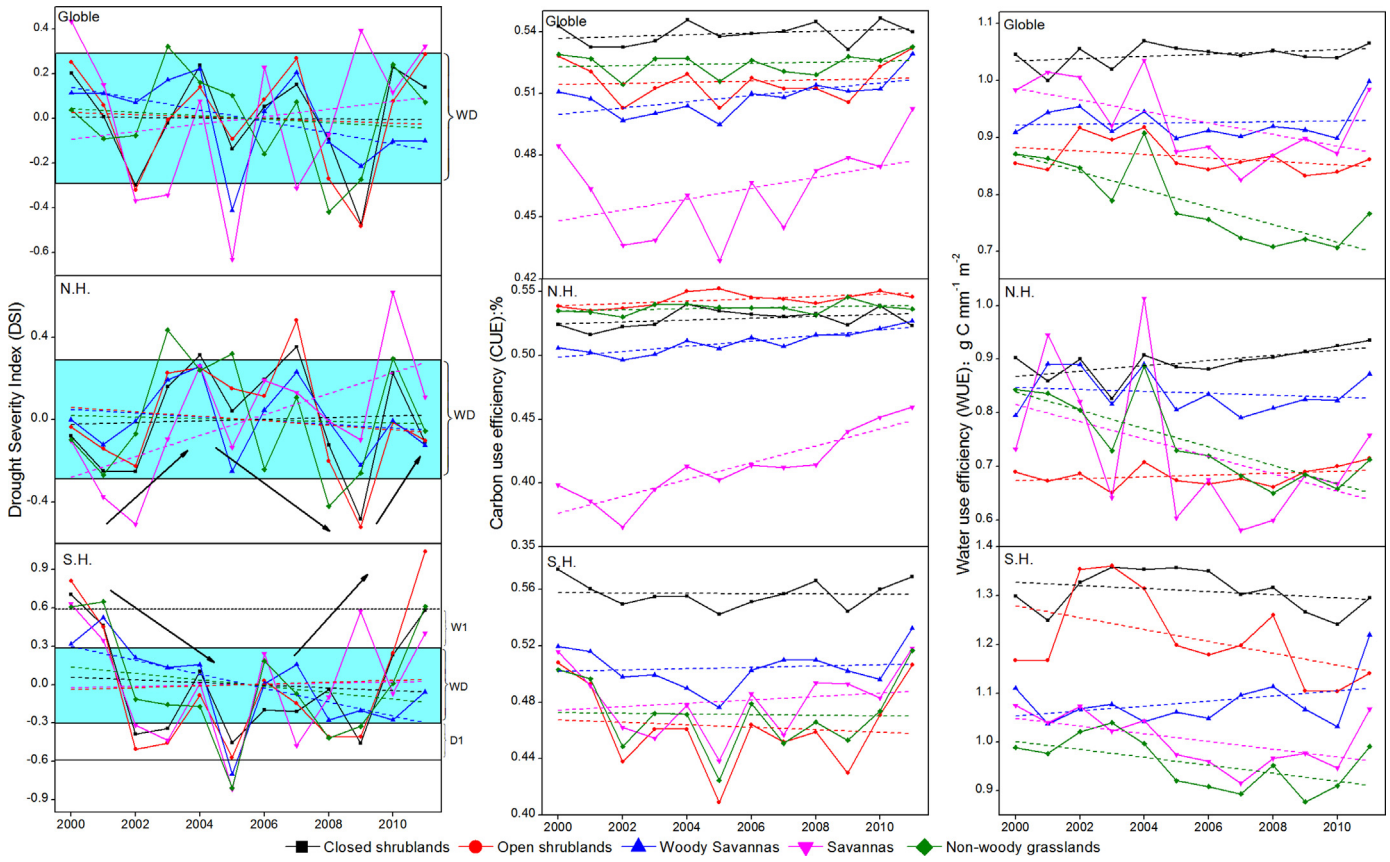

Fig. 4. The temporal dynamics of grassland DSI, CUE, and WUE from 2000 to 2011.

3.3. The correlations between grassland CUE, WUE and climatic variables

The correlations between grassland CUE, WUE and DSI, MAP, MAT were also calculated respectively to reveal the sensitivity of the grassland carbon and water use to climate variables. As shown in Fig. 5, the spatial pattern of correlation between grassland CUE and DSI was similar to that between grassland CUE and MAP but opposite to that between grassland CUE and MAT, particularly in the S.H. The regions with significant correlations (including extremely significant) between grassland CUE and DSI, MAP, MAT accounted for 52.92%, 20.14%, and 22.69% of the total grasslands, respectively. These regions are mainly located in Australia, southern Africa, western North America, and west of Asia. Generally, more than a half of grassland CUE was negatively correlated with DSI (53.53%) and MAT (68.68%), and positively correlated with MAP (68.71%). By contrast, the correlations between grassland WUE and climate variables were relatively low and presented significant spatial heterogeneity across the globe (Fig. 6). The regions with significant correlations between grassland WUE and DSI, MAP, MAT accounted for 22.11%, 12.96%, and 13.81% of the total grasslands, respectively. The regions that showed an extremely significant positive correlation between grassland WUE and DSI are mainly located in the Eurasia and the US Great Plains. Most of the grassland WUE was negatively correlated with DSI (56.06%) and MAP (56.58%), and positively correlated with MAT (53.38%).

4. Discussion

Climate change is expected to induce the geographic range and incidence of droughts, particularly in arid and semi-arid regions. These droughts are characterized by contractions and expansions and increasing and decreasing incidence. Recognizing how the carbon and water use of grassland ecosystems responds to these droughts can improve our understanding of the interactions between grassland carbon/water cycle and climate change. During the recent decade, most of grassland ecosystems in the N.H. were in near normal condition, but widespread droughts occurred around 2002 and 2009. These phenomena are consistent with those described in previous studies. Consecutive droughts were reported in South Asia in 2000–2003 (Pandey et al., 2007), and in North America in 2002 (Lawrimore and Stephens, 2003; Dong et al., 2011). The year 2005 was a turning point for the grassland ecosystems in the S.H., before this period, the dry spells expanded continually, and recovered in the following years (Watkins, 2005). Widespread drought also occurred in Australia from 2002 to 2003 (Horridge et al., 2005).

Droughts have adverse effects on ecosystems, especially those in regions where water supply is limited. In the N.H., the increase of CUE for each grassland type because of the increasing GPP and NPP fluctuated despite the occasional occurrence of droughts. These regions are mainly located in the northern high latitudes vegetated by the open shrublands, and some regions of the Mongolian Plateau covered by the non-woody grasslands. The decreased DSI value in these regions indicates a dry trend during the past decade. However, the grassland CUE showed an overall increasing trend in this period. The rising temperature in these regions probably promotes the photosynthesis process of grass, which resulted in more primary production (IPCC, 2012). In addition, the different sensitivities of NPP and GPP of each grassland type to the drought conditions are also likely contribute to the increase of CUE in these regions (Zhang et al., 2014). By contrast, droughts exerted significant impacts on

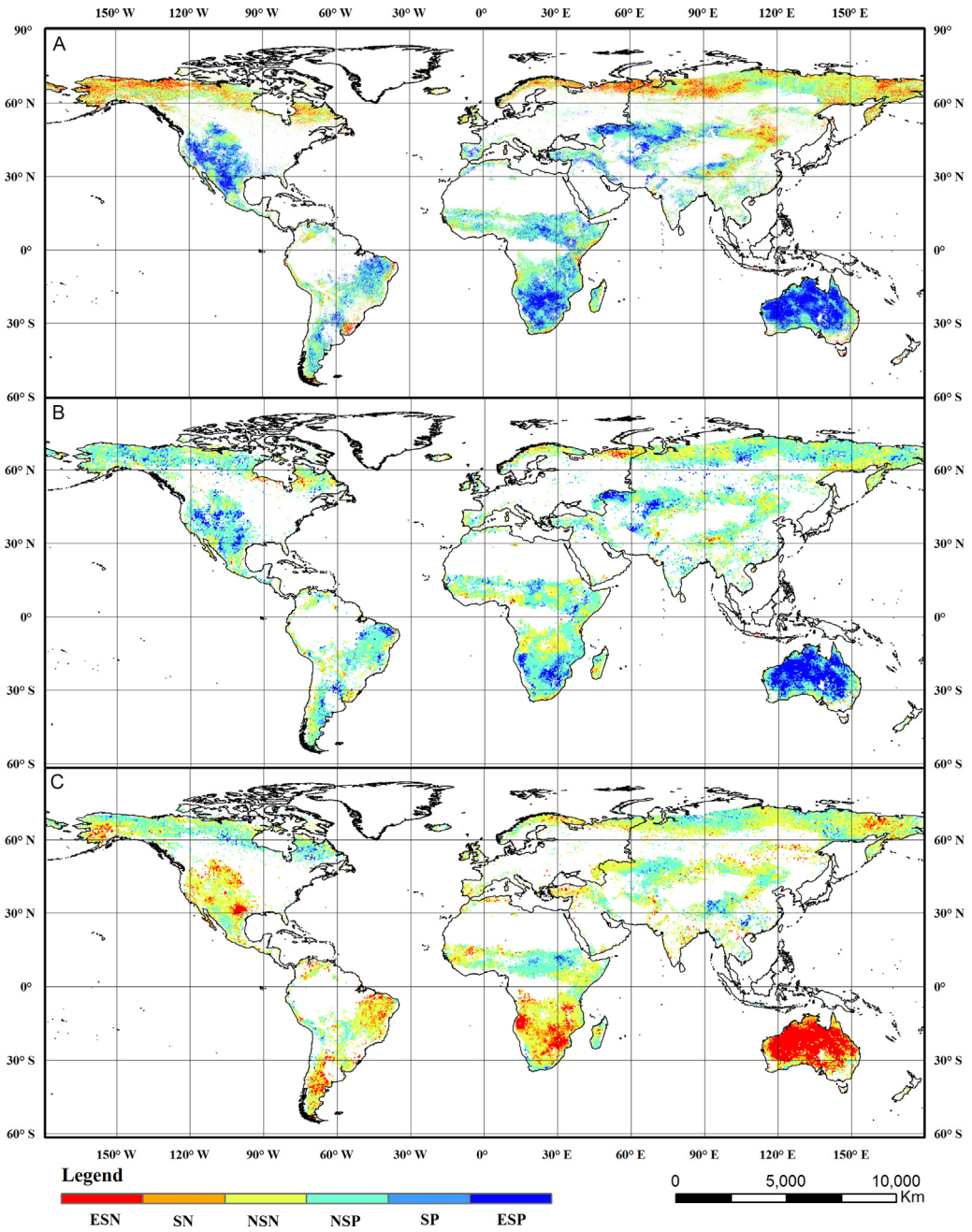

Fig. 5. The correlations between grassland CUE and DSI (A), MAP (B), and MAT (C). ESN: extremely significant negative; SN: significant negative; NSN: non-significant negative; NSP: non-significant positive; SP: significant positive; ESP: extremely significant positive.

grassland CUE in the S.H. Vegetation moisture constrains on canopy transpiration, as well as net photosynthesis, and CO_2 exchange (Mu et al., 2013). According to the calculation of DSI, lower NDVI values indicate the occurrence of drought. Under slight drought conditions, the net photosynthesis rate of grass decreases because of the decreased activity of ribulose diphosphate carboxylase and efficiency of the quantum yield of photosynthesis. These factors lead to the decrease in the photosynthetic capacity of mesophyll cells (Zhou et al., 2009). Soil water influences the response of Re and photosynthesis to temperature. The decreased rate of net photosynthesis under slight drought stress is induced by the progressive closure of leaf stoma, whereas that under severe drought conditions damages the photosynthetic organs of plants, thereby reducing plant water loss and photosynthesis (Arneth et al., 1998; Tian et al., 2009). CUE decreases in regions or time periods experiencing drought. This effect explains well the CUE dynamic in the S.H.

The correlation between grassland WUE and DSI was relatively low, thereby implying that grassland WUE was less sensitive to droughts than CUE at a global scale. Droughts induce an increase in plant WUE to mitigate the effects of water loss. Severer droughts enhance ecosystem resistance and resilience in responding to potential limits to water use, which likely contributed to the high WUE in the S.H. over the study period (Gang et al., 2015a,b). Variations in DSI exert a more considerably significant influence on WUE at the regional scale. The results of this study showed that grassland WUE was extremely significant positive correlated with DSI in the center of the Eurasia and parts of the US Great Plains,

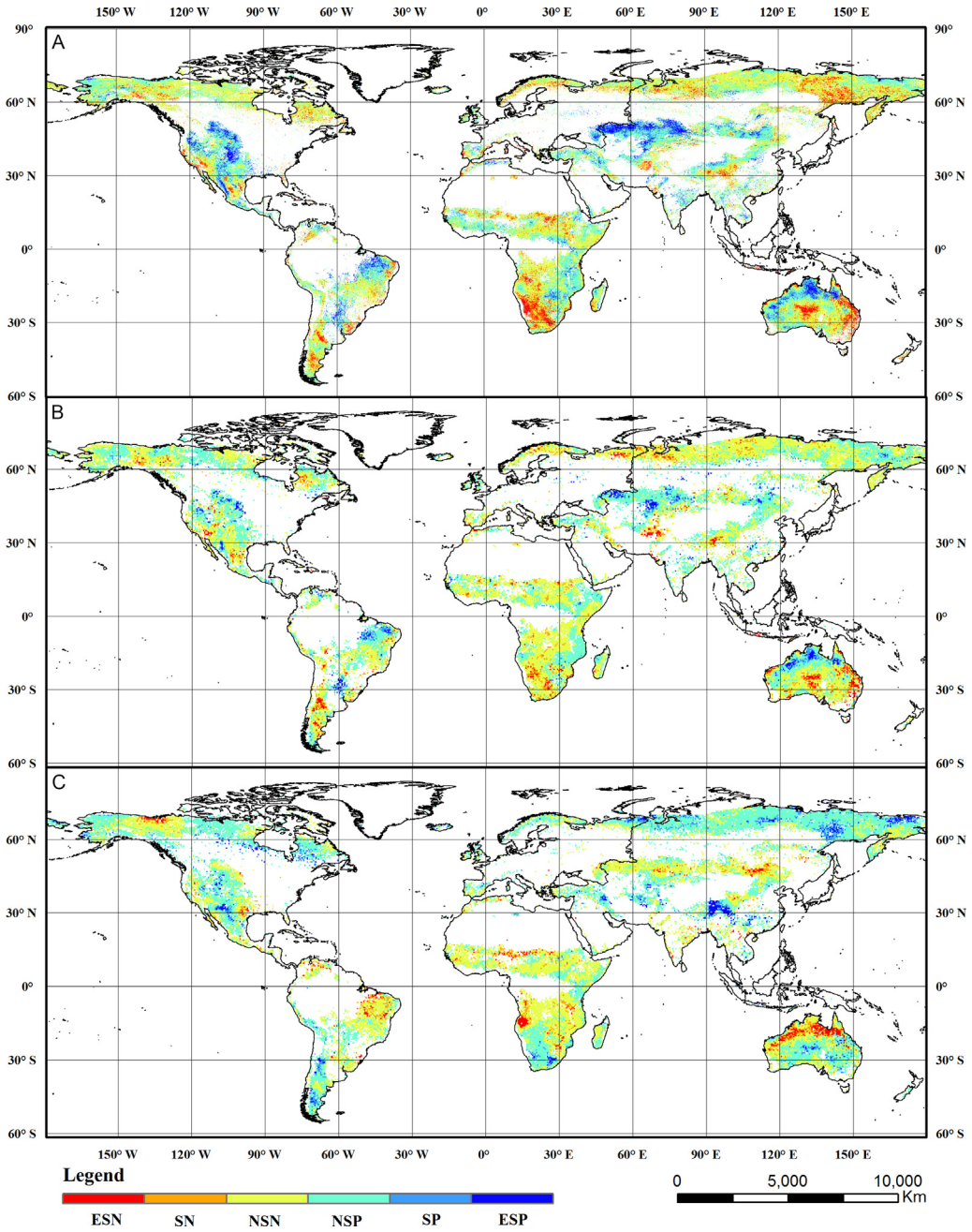

Fig. 6. The correlations between grassland WUE and DSI (A), MAP (B), and MAT (C). ESN: extremely significant negative; SN: significant negative; NSN: non-significant negative; NSP: non-significant positive; SP: significant positive; ESP: extremely significant positive.

where non-woody grasslands mostly vegetated. Plants with high WUE exhibit low photosynthesis rate, evapotranspiration rate, and stomatal conductance. The photosynthesis process can be maintained at a certain level even under severe drought conditions (Maroco et al., 2000; Ogaya and Peñuelas, 2003; Lefi et al., 2004; Zhang et al., 2005). By contrast, plants with low WUE are highly sensitive to rainfall conditions. Decreasing soil moisture decreases the rate of photosynthesis (Gebre et al., 1998; Zhang et al., 2005). Plants with high WUE can store more solutes than those with low WUE. These characteristics can partly explain the different responses of grassland types to droughts (Jiang and Dong, 1999; Reichstein et al., 2002; Chen et al., 2003). Given the limitation availability of data, only the correlations between the grassland DSI and CUE, and WUE over a 12-year period were examined in this study. Long-term information is needed to determine how grassland carbon and water use responds to drought conditions.

5. Conclusion

The recent climate change characterized by intensifying droughts threatens carbon sequestration and water use of grassland ecosystems. About 39.76% of the total grassland regions across the globe were in dry condition in 2000–2011. During this period, 57.04% of the grassland ecosystems became dry. The trend was mainly observed in the Asia, the north of North America, the southern Africa, and the Western Australia. Drought spells in grassland regions were more significant in the S. H. than in the N. H. In the N.H., most grassland ecosystems were in near normal condition.

Grassland CUE showed an overall increasing trend at the global scale despite the drought conditions. Specifically, it rose with fluctuation in the N.H. In the S.H., a clear drying and wetting trend was observed, with the year 2005 regarded as a turning point, during which all grassland types experienced drought. Droughts affect grassland CUE and WUE by influencing the photosynthesis and evapotranspiration process. The carbon and water use efficiencies of savannas were found to be most sensitive to droughts among all the grassland types. The DSI variation explains well of the temporal dynamic of grassland CUE over this period, particularly in the S. H. By contrast, the grassland WUE was less affected by the recent drought conditions at the global scale. However, the significance of droughts in WUE was highlighted when scaling down to regional scales. Overall, the carbon and water use of grasslands in the S.H. suffered more from the recent droughts in comparison with that in the N.H. These effects are likely to continue under the warming climate.

Conflict of interests

All the authors have no conflict of interests to declare.

Acknowledgements

This work was supported by the "The Doctroal Start-up Fund of Northwest A&F University (2452015339)", "APN Global Change Fund Project (No. ARCP2013-16NMY-LI)", "The National Program on Key Basic Research Project of China (973 Program, No. 2010CB950702)". We thank Prof. Jizhou Ren from Lanzhou University, Prof. Pavel Y. Groisman from the NOAA National Climatic Data Center for their guidance on the method and writing of this paper. We also appreciate the Numerical Terra dynamic Simulation Group (NTSG) and British Atmospheric Data Centre (BADC) for sharing datasets.

References

Adiredjo, A.L., Navaud, O., Muños, S., Langlade, N.B., Lamaze, T., Grieu, P., 2014. Genetic control of water use efficiency and leaf carbon isotope discrimination in sunflower (*Helianthus annuus* L.) subjected to two drought scenarios. PLOS ONE 9, e101218.

Arneth, A., Kelliher, F.M., McSeveny, T.M., Byers, J.N., 1998. Net ecosystem productivity, net primary productivity and ecosystem carbon sequestration in a *Pinus radiata* plantation subject to soil water deficit. Tree Physiol. 18, 785–793.

Atkinson, P.M., Dash, J., Jeganathan, C., 2011. Amazon vegetation greenness as measured by satellite sensors over the last decade. Geophys. Res. Lett., 38.

Battipaglia, G., De Micco, V., Brand, W.A., Saurer, M., Aronne, G., Linke, P., Cherubini, P., 2014. Drought impact on water use efficiency and intra-annual density fluctuations in *Erica arborea* on Elba (Italy). Plant Cell Environ. 37, 382–391.

Bollig, C., Feller, U., 2014. Impacts of drought stress on water relations and carbon assimilation in grassland species at different altitudes. Agric. Ecosyst. Environ. 188, 212–220.

Burri, S., Sturm, P., Prechsl, U.E., Knohl, A., Buchmann, N., 2014. The impact of extreme summer drought on the short-term carbon coupling of photosynthesis to soil CO_2 efflux in a temperate grassland. Biogeosciences 11, 961–975.

Chen, T., Meixue, Y., Shijian, F., Xu, H., Weiya, Q., Yuanging, H., Lizhe, A., 2003. Spatial distribution of stable carbon isotope compositions of plant leaves in the north of the Tibetan Plateau. J. Glaciol. Geocryol. 25, 83–87.

Ciais, P., Reichstein, M., Viovy, N., Granier, A., Ogée, J., Allard, V., Aubinet, M., Buchmann, N., Bernhofer, C., Carrara, A., 2005. Europe-wide reduction in primary productivity caused by the heat and drought in 2003. Nature 437, 529–533.

Delucia, E., Drake, J.E., Thomas, R.B., Gonzalez Meler, M., 2007. Forest carbon use efficiency: is respiration a constant fraction of gross primary production? Global Change Biol. 13, 1157–1167.

Dong, X., Xi, B., Kennedy, A., Feng, Z., Entin, J.K., Houser, P.R., Schiffer, R.A., L'Ecuyer, T., Olson, W.S., Hsu, K.L., 2011. Investigation of the 2006 drought and 2007 flood extremes at the Southern Great Plains through an integrative analysis of observations. J. Geophys. Res.: Atmos. 116 (D3).

French, N.R., 1979. Perspectives in grassland ecology. Springer-Verlag New York Inc.

Gang, C., Wang, Z., Zhou, W., Chen, Y., Li, J., Chen, J., Qi, J., Odeh, I., Groisman, P.Y., 2015a. Assessing the spatiotemporal dynamic of global grassland water use efficiency in response to climate change from 2000 to 2013. J. Agron. Crop Sci., http://dx.doi.org/10.1111/jac.12137.

Gang, C., Zhou, W., Wang, Z., Chen, Y., Li, J., Chen, J., Qi, J., Odeh, I., Groisman, P.Y., 2015b. Comparative assessment of grassland NPP dynamics in response to climate change in China, North America. Europe and Australia from 1981 to 2010. J. Agron. Crop Sci. 201, 57–68.

Gebre, G.M., Tschaplinski, T.J., Shirshac, T.L., 1998. Water relations of several hardwood species in response to throughfall manipulation in an upland oak forest during a wet year. Tree Physiol. 18, 299–305.

Harris, I., Jones, P.D., Osborn, T.J., Lister, D.H., 2014. Updated high resolution grids of monthly climatic observations – the CRU TS3. 10 Dataset. Int. J. Climatol. 34, 623–642.

Helmuth, B., Kingsolver, J.G., Carrington, E., 2005. Biophysics, physiological ecology, and climate change: does mechanism matter? Annu. Rev. Physiol. 67, 177–201.

Horridge, M., Madden, J., Wittwer, G., 2005. The impact of the 2002-2003 drought on Australia. J. Policy Model. 27, 285–308.

Huete, A., Didan, K., Miura, T., Rodriguez, E.P., Gao, X., Ferreira, L.G., 2002. Overview of the radiometric and biophysical performance of the MODIS vegetation indices. Remote Sens. Environ. 83, 195–213.

IPCC, 2007. Climate Change 2007: The Physical Scientific Basis. Cambridge University Press, Cambridge.

IPCC, 2012. Managing the risks of extreme events and disasters to advance climate change adaptation. A Special Report of Working Groups I and II of the Intergovernmental Panel on Climate Change. Cambridge University Press, Cambridge, UK, and New York, NY, USA, pp. 582.

Jiang, G., Dong, M., 1999. A comparative study on photosynthesis and water use efficiency between clonal and non-clonal plant species along the Northeast China Transect (NECT). Acta Botan. Sin. 42, 855–863.

Jung, V., Albert, C.H., Violle, C., Kunstler, G., Loucougaray, G., Spiegelberger, T., 2014. Intraspecific trait variability mediates the response of subalpine grassland communities to extreme drought events. J. Ecol. 102, 45–53.

Justice, C.O., Townshend, J., Vermote, E.F., Masuoka, E., Wolfe, R.E., Saleous, N., Roy, D.P., Morisette, J.T., 2002. An overview of MODIS Land data processing and product status. Remote Sens. Environ. 83, 3–15.

Keenan, T.F., Hollinger, D.Y., Bohrer, G., Dragoni, D., Munger, J.W., Schmid, H.P., Richardson, A.D., 2013. Increase in forest water-use efficiency as atmospheric carbon dioxide concentrations rise. Nature 499, 324–327.

Koerner, S.E., Collins, S.L., 2014. Interactive effects of grazing, drought, and fire on grassland plant communities in North America and South Africa. Ecology 95, 98–109.

Lawrimore, J., Stephens, S., 2003. Climate of 2002 annual review. NOAA National Climatic Data Center, Available online at http://lwf.ncdc.noaa.gov/oa/climate/research/2002/ann/events.html.

Lefi, E., Medrano, H., Cifre, J., 2004. Water uptake dynamics, photosynthesis and water use efficiency in field-grown *Medicago arborea* and *Medicago citrina* under prolonged Mediterranean drought conditions. Ann. Appl. Biol. 144, 299–308.

LeHouerou, H.N., 1984. Rain use efficiency: a unifying concept in arid-land ecology. J. Arid Environ. 7, 213–247.

Loveland, T.R., Reed, B.C., Brown, J.F., Ohlen, D.O., Zhu, Z., Yang, L., Merchant, J.W., 2000. Development of a global land cover characteristics database and IGBP DISCover from 1 km AVHRR data. Int. J. Remote Sens. 21, 1303–1330.

Manea, A., Leishman, M.R., 2014. Leaf area index drives soil water availability and extreme drought-related mortality under elevated CO_2 in a temperate grassland model system. PLOS ONE 9, e91046.

Maroco, J.P., Pereira, J.S., Chaves, M.M., 2000. Growth, photosynthesis and water-use efficiency of two C 4 Sahelian grasses subjected to water deficits. J. Arid Environ. 45, 119–137.

McKee, T.B., Doesken, N.J., Kleist, J.,1995. Drought monitoring with multiple time scales. In: Ninth Conference on Applied Climatology. American Meteorological Society, Boston, pp. 233–236.

Monteith, J.L., 1965. Evaporation and environment. Symp. Soc. Exp. Biol., 205–234.

Mu, Q., Heinsch, F.A., Zhao, M., Running, S.W., 2007a. Development of a global evapotranspiration algorithm based on MODIS and global meteorology data. Remote Sens. Environ. 111, 519–536.

Mu, Q., Zhao, M., Heinsch, F.A., Liu, M., Tian, H., Running, S.W., 2007b. Evaluating water stress controls on primary production in biogeochemical and remote sensing based models. J. Geophys. Res. 112 (G1).

Mu, Q., Zhao, M., Kimball, J.S., McDowell, N.G., Running, S.W., 2013. A remotely sensed global terrestrial drought severity index. Bull. Am. Meteorol. Soc. 94, 83–98.

Mu, Q., Zhao, M., Running, S.W., 2011. Improvements to a MODIS global terrestrial evapotranspiration algorithm. Remote Sens. Environ. 115, 1781–1800.

Ogaya, R., Peñuelas, J., 2003. Comparative field study of *Quercus ilex* and *Phillyrea latifolia*: photosynthetic response to experimental drought conditions. Environ. Exp. Bot. 50, 137–148.

O'Mara, F.P., 2012. The role of grasslands in food security and climate change. Ann. Bot. -Lond. 110, 1263–1270.

Palmer, W.C., 1965. Meteorological Drought. US Department of Commerce, Weather Bureau, Washington, DC, USA.

Pandey, S., Bhandari, H.S., Hardy, B., 2007. Economic costs of drought and rice farmers' coping mechanisms: a cross-country comparative analysis. Int. Rice Res. Inst., 203.

Reichstein, M., Tenhunen, J.D., Roupsard, O., Ourcival, J.M., Rambal, S., Miglietta, F., Peressotti, A., Pecchiari, M., Tirone, G., Valentini, R., 2002. Severe drought effects on ecosystem CO_2 and H_2O fluxes at three Mediterranean evergreen sites: revision of current hypotheses? Global Change Biol. 8, 999–1017.

Rosegrant, M.W., Cai, X., Cline, S.A., 2003. Will the world run dry? Global water and food security. Environ.: Sci. Policy Sustain. Dev. 45, 24–36.

Rowland, L., Hill, T.C., Stahl, C., Siebicke, L., Burban, B., Zaragoza-Castells, J., Ponton, S., Bonal, D., Meir, P., Williams, M., 2014. Evidence for strong seasonality in the carbon storage and carbon use efficiency of an Amazonian forest. Global Change Biol. 20, 979–991.

Sandholt, I., Rasmussen, K., Andersen, J., 2002. A simple interpretation of the surface temperature/vegetation index space for assessment of surface moisture status. Remote Sens. Environ. 79, 213–224.

Scurlock, J., Hall, D.O., 1998. The global carbon sink: a grassland perspective. Global Change Biol. 4, 229–233.

Shakya, N., Yamaguchi, Y., 2010. Vegetation, water and thermal stress index for study of drought in Nepal and central northeastern India. Int. J. Remote Sens. 31, 903–912.

Tian, Y.Q., Gao, Q., Zhang, Z.C., Zhang, Y., Zhu, K., 2009. The advances in study on plant photosynthesis and soil respiration of alpine grasslands on the Tibetan Plateau. Ecol. Environ. Sci. 18, 711–721.

Van der Molen, M.K., Dolman, A.J., Ciais, P., Eglin, T., Gobron, N., Law, B.E., Meir, P., Peters, W., Phillips, O.L., Reichstein, M., 2011. Drought and ecosystem carbon cycling. Agric. Forest Meteorol. 151, 765–773.

Vörösmarty, C.J., Green, P., Salisbury, J., Lammers, R.B., 2000. Global water resources: vulnerability from climate change and population growth. Science 289, 284–288.

Watkins, A.B., 2005. The Australian drought of 2005. WMO Bull. 54, 1–7.

Webb, W., Szarek, S., Lauenroth, W., Kinerson, R., Smith, M., 1978. Primary productivity and water use in native forest, grassland, and desert ecosystems. Ecology 59, 1239–1247.

White, R.P., Murray, S., Rohweder, M., Prince, S.D., Thompson, K.M., 2000. Grassland Ecosystems. World Resources Institute, Washington, DC, USA.

Wolf, S., Eugster, W., Ammann, C., Häni, M., Zielis, S., Hiller, R., Stieger, J., Imer, D., Merbold, L., Buchmann, N., 2013. Contrasting response of grassland versus forest carbon and water fluxes to spring drought in Switzerland. Environ. Res. Lett. 8, 35007.

Zhang, X., Wu, N., Li, C., 2005. Physiological and growth responses of *Populus davidiana* ecotypes to different soil water contents. J. Arid Environ. 60, 567–579.

Zhang, X.Q., Yamaguchi, Y., 2014. Characterization and evaluation of MODIS-derived Drought Severity Index (DSI) for monitoring the 2009/2010 drought over southwestern China. Nat. Hazards 74, 2129–2145.

Zhang, Y., Yu, G., Yang, J., Wimberly, M.C., Zhang, X., Tao, J., Jiang, Y., Zhu, J., 2014. Climate-driven global changes in carbon use efficiency. Global Ecol. Biogeogr. 23, 144–155.

Zhao, M., Heinsch, F.A., Nemani, R.R., Running, S.W., 2005. Improvements of the MODIS terrestrial gross and net primary production global data set. Remote Sens. Environ. 95, 164–176.

Zhao, M., Running, S.W., 2010. Drought-induced reduction in global terrestrial net primary production from 2000 through 2009. Science 329, 940–943.

Zhao, M., Running, S.W., 2011. Response to comments on "Drought-induced reduction in global terrestrial net primary production from 2000 through 2009". Science 333, 1093.

Zhao, M., Running, S.W., Nemani, R.R., 2006. Sensitivity of Moderate Resolution Imaging Spectroradiometer (MODIS) terrestrial primary production to the accuracy of meteorological reanalyses. J. Geophys. Res. 111 (G1).

Zhou, Q.P., Cheng, J.M., Wan, H.E., Yu, J., 2009. Study on the diurnal variations of photosynthetic characteristics and water use efficiency of *Stipa bungeana Trin.* under drought stress. Acta Agrectir Sin. 17, 510–514.